Liposomal dexamethasone inhibits tumor growth in an advanced human-mouse hybrid model of multiple myeloma

Anil K. Deshantri[a,b], Marcel H. Fens[a,c], Ruud W.J. Ruiter[d], Josbert M. Metselaar[e,f], Gert Storm[c,g], Louis van Bloois[c], Aida Varela-Moreira[a,c], Sanjay N. Mandhane[b], Tuna Mutis[d], Anton C.M. Martens[d], Richard W.J. Groen[d], Raymond M. Schiffelers[a,c,*]

[a] Department of Clinical Chemistry and Hematology, University Medical Center Utrecht, Utrecht, The Netherlands
[b] Biological Research Pharmacology Department, Sun Pharma Advanced Research Company Ltd., Vadodara, India
[c] Department of Pharmaceutics, Utrecht Institute for Pharmaceutical Sciences, Utrecht University, Utrecht, The Netherlands
[d] Department of Hematology, Amsterdam UMC, VU University Medical Center, Cancer Center Amsterdam, Amsterdam, The Netherlands
[e] Enceladus Pharmaceuticals, Naarden, The Netherlands
[f] Department of Experimental Molecular Imaging, University Clinic and Helmholtz Institute for Biomedical Engineering, RWTH-Aachen University, Aachen, Germany
[g] Department of Biomaterials Science and Technology, University of Twente, Enschede, The Netherlands

ARTICLE INFO

ABSTRACT

Glucocorticoids are the cornerstone in the clinic for treatment of hematological malignancies, including multiple myeloma. Nevertheless, poor pharmacokinetic properties of glucocorticoids require high and frequent dosing with the off-target adverse effects defining the maximum dose. Recently, nanomedicine formulations of glucocorticoids have been developed that improve the pharmacokinetic profile, limit adverse effects and improve solid tumor accumulation. Multiple myeloma is a hematological malignancy characterized by uncontrolled growth of plasma cells. These tumors initiate increased angiogenesis and microvessel density in the bone marrow, which might be exploited using nanomedicines, such as liposomes. Nano-sized particles can accumulate as a result of the increased vascular leakiness at the bone marrow tumor lesions. Pre-clinical screening of novel anti-myeloma therapeutics *in vivo* requires a suitable animal model that represents key features of the disease. In this study, we show that fluorescently labeled long circulating liposomes were found in plasma up to 24 h after injection in an advanced human-mouse hybrid model of multiple myeloma. Besides the organs involved in clearance, liposomes were also found to accumulate in tumor bearing human-bone scaffolds. The therapeutic efficacy of liposomal dexamethasone phosphate was evaluated in this model showing strong tumor growth inhibition while free drug being ineffective at an equivalent dose (4 mg/kg) regimen. The liposomal formulation slightly reduced total body weight of myeloma-bearing mice during the course of treatment, which appeared reversible when treatment was stopped. Liposomal dexamethasone could be further developed as monotherapy or could fit in with existing therapy regimens to improve therapeutic outcomes for multiple myeloma.

1. Introduction

Multiple myeloma is a hematological malignancy that originates in bone marrow and is characterized by clonal proliferation of a single plasma cell resulting in monoclonal immunoglobulin production [1]. Steroidal anti-inflammatory drugs, like glucocorticoids (GCs), are important in the treatment of a variety of cancers including hematological malignancies [2–6]. GCs are potent drugs with both anti-inflammatory and anti-angiogenic properties [4]. At lower concentrations, GCs enhance production of anti-inflammatory proteins/cytokines (transactivation), while at higher concentrations they inhibit production of pro-inflammatory cytokines (transrepression) [7]. The anti-tumor efficacy of GCs is a result of a combination of these two effects as well as the apoptosis caused by direct cell lysis [2,8]. Dexamethasone is used in the clinic for the treatment of various types of inflammatory driven malignancies including multiple myeloma [9]. In regimens used to treat patients suffering from MM, dexamethasone is typically combined with other chemotherapeutic agents such as proteasome inhibitors (bortezomib and carfilzomib), immune modulators (thalidomide and lenalidomide), and cyclophosphamide or melphalan [9].

Dexamethasone has shown to improve clinical outcomes in MM patients when part of the treatment regimens [10–13]. However, GCs have off-target adverse effects like strong systemic immunosuppression, which can lead to opportunistic infections which, when not treated successfully, can result in death [2]. Other side effects of GCs include osteoporosis, osteonecrosis, myopathy, growth suppression in children, hypertension, rapid weight gain, fat redistribution, diabetes, hypertriglyceridemia, hypercholesterolemia, adrenal insufficiency, skin thickening, glaucoma, cataract, peptic ulcer disease, decelerated wound healing, and electrolyte imbalance [14–17]. Moreover, GCs have poor pharmacokinetic profiles (i.e. rapid clearance and large volume of distribution after injection). This requires high and frequent dosing [8]. Liposomal encapsulation of anti-inflammatory and anti-cancer drugs has proven to be an effective method to improve therapeutic outcomes in inflamed tissues and solid tumors [2,6,15,18,19]. Liposomal encapsulation of dexamethasone has been shown to enhance local concentrations in inflamed tissues, while reducing exposure to toxicity-sensitive organs. Previously, we have shown substantial efficacy of long circulating liposomal prednisolone phosphate (LCL-PLP) in solid syngeneic/xenograft tumor models such as B16F10 melanoma and C26 colon carcinoma [6]. Tumor growth inhibition was also found to be superior in LCL-PLP treated mice in an advanced mouse model of spontaneous mammary carcinoma [2]. Interestingly, LCL-PLP showed significant accumulation into the tumor tissues despite the slow tumor growth kinetics in the latter more clinically relevant model [2].

In general, the enhanced permeability and retention (EPR) effect has been ascribed to apply to palpable solid tumors in which angiogenesis is intensive and facilitating rapid tumor growth [20]. Nevertheless, a growing body of evidence supports the presence of angiogenesis and increased microvessel density in hematological malignancies including multiple myeloma [21–23]. Therefore, targeted drug delivery using nanocarrier systems such as liposomes potentially increases the local drug concentration at the myeloma lesions, thereby improving the therapeutic index of GCs. Importantly, in multiple myeloma the bone marrow (BM) microenvironment is of crucial importance and cannot be ignored when studying anti-myeloma therapies *in vivo*. The interaction of malignant cells with bone marrow stromal cells plays a crucial role in proliferation and survival of the malignant cells [24–29]. Therefore, an animal model is required that not only appreciates the role of increased angiogenesis but also harbors the crucial interaction of myeloma cells and surrounding cells in the BM microenvironment. Previously, we have described an advanced mouse model for multiple myeloma [30,31]. In this human-mouse hybrid model, human bone-like environments are introduced subcutaneously in immunodeficient RAG2$^{-/-}$γc$^{-/-}$ mice. These bone-like structures are generated through seeding and subsequent differentiation towards the osteogenic lineage of human mesenchymal stromal cells (MSCs) on biphasic calcium phosphate. Vascularization in and around the scaffolds could be seen by histopathological analysis. After formation of the human bone, multiple myeloma cells are inoculated in the scaffolds. This human-mouse hybrid animal model has shown to closely resemble the actual disease and to accurately predict individual patient response in a personalized treatment set-up [30]. In the present study, using this model, we investigated circulation times and biodistribution of fluorescently labeled long circulating liposomes. Furthermore, the therapeutic potential of liposomal dexamethasone (LCL-DEX) was evaluated, revealing that liposomal encapsulation strongly increased the therapeutic efficacy.

2. Materials and methods

2.1. Liposome assembly

2.1.1. Long circulating Alexa750 labeled liposomes (LCL-Alexa)
PEGylated liposomes were prepared by lipid film hydration method as described previously [2]. In short, appropriate amounts of dipalmitoylphosphatidylcholine (DPPC), poly (ethylene glycol) 2000-distearoylphosphatidylethanolamine (PEG(2000)-DSPE) (both from Lipoid GmbH, Germany), and cholesterol (Sigma Aldrich, Germany) were dissolved in chloroform in a molar percentage of 50%, 5%, and 45% respectively. A lipid film was prepared under reduced pressure on a rotary evaporator and dried under a stream of nitrogen. The lipid film was subsequently hydrated with HEPES buffered saline (HBS) at pH 7.4. The liposome dispersion was then extruded 10 times with high pressure extruder (Lipex, Northern Lipids) equipped with two stacked polycarbonate membrane filters with 100 nm pores. Liposomes were stored at 4 °C until use. Alexa750 liposomes (LCL-Alexa) were obtained by post insertion of Alexa750 labeled PEG(2000)-DSPE micelles as described previously [32,33]. For micelles preparation, PEG(2000)-DSPE-NH$_2$ and PEG(2000)-DSPE (Avanti Polar Lipids, Birmingham, AL, USA) were mixed in a 1:1 M ratio in 0.1 M sodium bicarbonate solution at pH 8.3. This mixture was then heated at 60 °C for 10 min. 1 mg of Alexa-750 succinimidyl (Invitrogen, Carlsbad, CA, USA) was added to 0.5 mL of PEG(2000)-DSPE micelles, which led to coupling of Alexa750 to the NH$_2$-PEGylated lipid. Subsequently, the Alexa750 labeled micelles were added to the liposomes and mixed under repeated temperature cycling between 60 °C and room temperature, allowing the PEGylated and Alexa750-conjugated lipids to insert into the liposome bilayer.

2.1.2. Liposomal dexamethasone (LCL-DEX)
Dexamethasone phosphate PEG-liposomes were prepared using the ethanol injection method as described previously [34]. 1 mL of an alcoholic lipid solution DPPC, PEG(2000)-DSPE (both from Lipoid GmbH, Germany), and cholesterol (Sigma Aldrich, Germany) in a molar percentage of 62.5%, 4.8%, and 32.7% of total lipid content, respectively, was injected in 9 mL of an aqueous solution of 100 mg/mL dexamethasone phosphate disodium salt (Fagron, The Netherlands). Subsequently, the 10 mL crude liposome dispersion was sized by multiple extrusions at 60 °C using a medium pressure extruder (Lipex, Northern Lipids) equipped with two stacked polycarbonate membrane filters with 100 nm pores. Alcohol and non-encapsulated dexamethasone phosphate were removed by ultrafiltration and replacement of the filtrate with clean phosphate buffered 0.9% saline (pH 7.4). Lipid content was determined using high performance liquid chromatography coupled to an evaporative light scattering detector (HPLC-ELSD, Alltech 2000, Buchi, Switzerland) as described previously [35]. Separations were performed by an Astec® diol bonded silica normal phase column (250 mm × 4.6 I.D., particle size 5.0 μm, Sigma Aldrich, Germany). Eluents used were (i) 60% dichloromethane, 34% methanol, 1% ammonium hydroxide, 5% water (v/v) (mobile phase A), and (ii) 91% dichloromethane, 8% methanol: 1% ammonium hydroxide (v/v) (mobile phase B). A linear gradient was applied starting with 100% (v/v) mobile phase B changing to 80% mobile phase A: 20% mobile phase B at 11 min. The gradient was maintained at 80% mobile phase A and 20% mobile phase B for 5 min and changed to 100% mobile phase A after 16 min. The total run time was 30 min at 1 mL/min. Injection volume was 20 μL. ELSD settings included a gain of 15, tube temperature of 71 °C and a pressure of 28 psi. The column was maintained at ambient temperature. The retention time for DPPC and DSPE-PEG was approximately 15 min and 9 min, respectively. Response factor of the standards (prepared in mobile phase B in the range of 0.05–1.0 mg/mL) was calculated using log concentration and log peak area. Standard curves of DPPC and DSPE-PEG were prepared in mobile phase B. Liposomal dexamethasone was diluted in mobile phase B. The amount of dexamethasone phosphate encapsulated was determined as described previously [36]. In brief, a chloroform-methanol extraction was performed to the liposomes. Dexamethasone content was determined in the aqueous phase by ultra-high performance liquid chromatography (UPLC) (Waters Corporation, USA) using a C18 column (ACQUITYUPLC®BEHC18 1.7 μm, 2.1 × 50 mm). Liposomes were diluted and dissolved in 25% acetonitrile in HBS. As solution of 25% acetonitrile and 75% water at pH 2 (adjusted by addition of perchloric acid) was used as

mobile phase. Flow rate was set at 1 mL/min with an injection volume of 7.5 μL. Absorbance was detected at 254 nm and the run time was set as 1 min.

2.2. In vitro efficacy of LCL-DEX

Luciferase gene transfected multiple myeloma cell line MM.1S was used for *in vitro* efficacy experiments. Cells were cultured in 6-well plates in the presence of RPMI medium supplemented with 10% fetal calf serum, and 1% penicillin/streptomycin (all three from Life Technologies, USA). For cytotoxicity assays, cells were seeded in Greiner CELLSTAR® 96-well plates (Sigma Aldrich), with a density of 6250 cells per well. After culturing for 24 h, cells were treated in triplicates with increasing concentrations of free dexamethasone (Free-DEX) or LCL-DEX. After 48 h of incubation at 37 °C and 5% CO_2, beetle luciferin (Promega, US) was added in each well at a final concentration of 3 mM. Ten minutes after addition of luciferin, the plates were read for luminescence (SpectraMax M2e, Molecular Devices, Canada). Percentage viability was determined compared to control (untreated) wells.

2.3. Animal experiments

All animal experiments were conducted after acquiring permission from the local ethical committee for animal experimentation and were in compliance with the Dutch Animal Experimentation Act. Female $RAG2^{-/-}\gamma c^{-/-}$ mice were used for the study. Mice were kept in standard housing on a 12 h light/dark cycle. Standard rodent chow diet and water was provided ad libitum. Human bone-like scaffolds were created as described previously [30,31]. In short, 4 hybrid scaffolds consisting of three 2- to 3-mm biphasic calcium phosphate particles loaded with human MSCs were implanted subcutaneously into the back side of $RAG2^{-/-}\gamma c^{-/-}$ mice. Eight weeks after implantation, animal were irradiated with γ-rays (± 5 min, dose 1.5 Gy). Next day, scaffolds were inoculated with MM.1S cells (0.5×10^6 cells/scaffold) with prior viral gene transfection with a luciferase-containing construct. Treatments were started 12 days after tumor cell inoculation.

2.3.1. Circulation kinetics and biodistribution of fluorescently labeled liposomes

For circulation and biodistribution of fluorescently labeled liposomes, animals received a single intravenous (i.v.) injection of 5 mL/kg LCL-Alexa (total lipids at approximately 0.6 mmol/kg; Alexa750 at 400 μg/kg). From each animal, blood was withdrawn at three time points. At first two time points (i.e. at 1 min, and 1 h or 2 h), blood (± 50 μL) was withdrawn via submandibular puncture. At the third time point (i.e. at 4 h or 24 h), blood sampling was performed via cardiac puncture directly after animals were sacrificed by CO_2 asphyxia. Plasma was collected by centrifuging the blood samples at 1000 x g at 4 °C for 10 min and stored at −20 °C until further analysis. Tumor bearing scaffolds and organs (lungs, kidneys, liver, spleen, femurs, sternum, heart and brain) were collected, imaged for whole organ fluorescence (Biospace Lab Photon Imager, Meyer instrument, USA), fixed in liquid nitrogen or formalin and stored at −80 °C or room temperature, respectively, until further processing.

Fluorescence in plasma and tissue homogenates was analyzed by Odyssey fluorescence scanner (Westburg, Netherlands). A calibration curve was prepared and analyzed with spiked concentrations of Alexa750-labeled liposomes in mouse plasma. Pieces of the frozen tissues were weighed and homogenized in RIPA buffer (100 μL/100 mg tissue) using a bead mill homogenizer (60 s at 6000 rotation speed on a Precellys 24, Bertin Instruments, France). Next, homogenates were vortexed and centrifuged (12,000 x g for 10 min at 4 °C). Finally, supernatants were analyzed for fluorescence by Odyssey fluorescence scanner.

Femurs and sternums, that were formalin fixed for 24–48 h, and

decalcified for two weeks in 14% EDTA solution followed by snap freezing in liquid nitrogen, together with the yet in liquid nitrogen stored tissue samples, were cryosectioned with 5 μm thickness. After methanol (100%) fixation for 15 min, nuclei were stained with HOECHST 33342 (1 μg/mL for 15 min at RT) and the actin cytoskeleton was stained using phalloidin-Alexa 488 (1:30 for 45 min at RT). The slides were imaged using a Nikon Eclipse Ti-E widefield microscope equipped with a 60 × 1.49NA Nikon oil objective. A perfect focus module was used to retain sample focus during the measurements. A mercury arc lamp in conjunction with proper illumination and detection wavelength optics for the specific dyes was used; for Hoechst staining, a 330–380 nm excitation filter, a 400 nm longpass dichroic mirror and a 420 nm longpass emission filter (Nikon UV-2A filterset), for Alexa488 staining, a 450–490 nm excitation filter, a 505 nm longpass dichroic mirror and a 520 nm longpass emission filter (Nikon B-2A filterset), and for Alexa 750-labeled liposomes, a 690–730 nm excitation filter, a 741 nm longpass dichroic mirror and a 750–800 nm emission filter (Semrock Cy7-A-NTE-ZERO filterset). Finally, an Andor NEO sCMOS camera was used to record the images. Images were analyzed using ImageJ software version 10.2.

2.3.2. In vivo efficacy of LCL-DEX in a human-mouse hybrid model for MM

Artificial human bone-like scaffolds were developed in $RAG2^{-/-}\gamma c^{-/-}$ mice as described above. Treatments were initiated after 12 days of MM.1S cells inoculation. Bioluminescence imaging (BLI) (Photon Imager; Biospace Laboratory,) was performed just before start of the treatments (i.e. day 0). On the basis of BLI signals on day 0, animals were randomized into different treatment groups: phosphate buffered saline (PBS) (*n* = 11), PBS-liposomes (*n* = 4), Free-DEX at 1 and 4 mg/kg (n = 4 and *n* = 8, respectively), and LCL-DEX at 1 and 4 mg/kg (*n* = 4 and n = 8, respectively). All treatments were given i.v. via tail vein twice weekly, at a total of 5 injections. The experimental design is depicted in Fig. 1.

BLI was performed once weekly up to four weeks from start of the treatment. Body weight of animals was measured in order to monitor systemic toxicity associated with the treatments. Animals were sacrificed when they reached humane endpoint i.e. cumulative tumor volume > 10% of body weight (measured by digital caliper, Mitutoyo, Japan) or at the set endpoints of the experiment.

2.4. Statistical analysis

Data of *in vitro* cytotoxicity experiments was analyzed by GraphPad prism version 7.02 by using the non-linear regression method. Fluorescence intensity data in plasma samples obtained by Odyssey florescence scanner were analyzed by PKsolver version 2.0 to estimate time required for one half of the total amount of fluorescence intensity (thus liposomes) to be cleared from the circulation ($t^{1/2}$). Bioluminescence images were analyzed by Biospace Lab Photo Acquisition software version 2.9 (Meyer instrument, USA). Data obtained from the software was presented at counts per minute/square centimeters (cpm/cm^2). Percentage tumor growth in each treatment group was calculated relative to day 0, and was analyzed by GraphPad prism version 7.02 utilizing nonlinear regression using exponential growth eq. $Y = Y_0 \times exp.(k \times X)$. Where Y_0 is the Y value when X (time) is zero and k is the rate constant. Tumor doubling times for each group were used as a measure of relative tumor growth.

3. Results

3.1. Characterization of liposomes

The average diameter of LCL-Alexa was 122 ± 2 nm with a polydispersity index (PDI) 0.07 ± 0.01 as measured by dynamic light scattering. The amount of Alexa750 was 80 μg/mL and the liposomes contained 80.5 ± 3.4 mg total lipids/mL. The mean diameter of LCL-
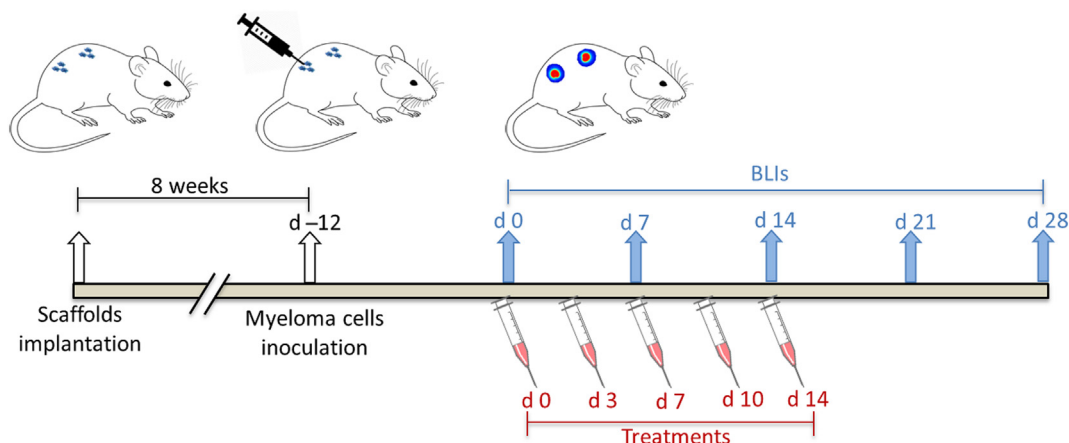
Fig. 1. Experimental design of therapeutic efficacy *in vivo* studies. Twelve days after MM.1S cell inoculations into 4 separate scaffolds per mouse, animals were randomized based on baseline BLI signals on day 0. Animals were treated twice weekly for a total of 5 injections (i.e. day 0, 3, 7, 10 and 14). BLI was performed on the day of first injection (day 0) followed by once weekly up to 4 weeks after treatment initiation. BLI = Bioluminescence imaging.

DEX was 113 ± 0.9 nm with a mean PDI of 0.116 ± 0.02. The surface charge was -11 ± 1 mV. The liposomes contained 0.95 ± 0.03 mg dexamethasone phosphate/mL and 50 mg total lipid/mL.
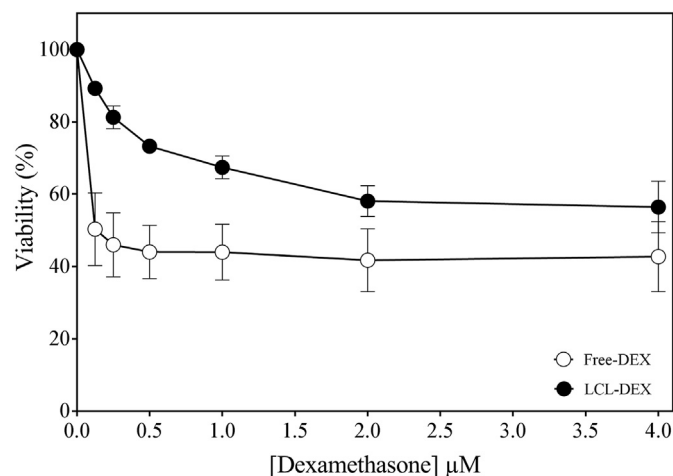
3.2. In vitro efficacy of LCL-DEX

In the *in vitro* cytotoxicity assays using the MM.1S cell line performed by measuring bioluminescence, we saw a concentration-dependent inhibition of cell proliferation after incubation with Free-DEX as well as LCL-DEX. The maximum inhibition was found to be approximately 60% and 45% in case of Free-DEX and LCL-DEX, respectively. Free-DEX showed 12 times higher efficacy as compared to LCL-DEX. The 50% inhibitory concentration (IC_{50}) was $0.41\,\mu$M (95% CI = 0.22–0.76) and $5.02\,\mu$M (95% CI = 3.71–7.49) for Free-DEX and LCL-DEX, respectively, making Free-DEX ~12 times more efficacious (Fig. 2).

3.3. Plasma levels and tissue distribution of fluorescently labeled liposomes

The level of fluorescence in plasma samples, collected at different time points after LCL-Alexa were administered i.v. to tumor scaffolds-bearing mice, was measured. Immediately after administration of
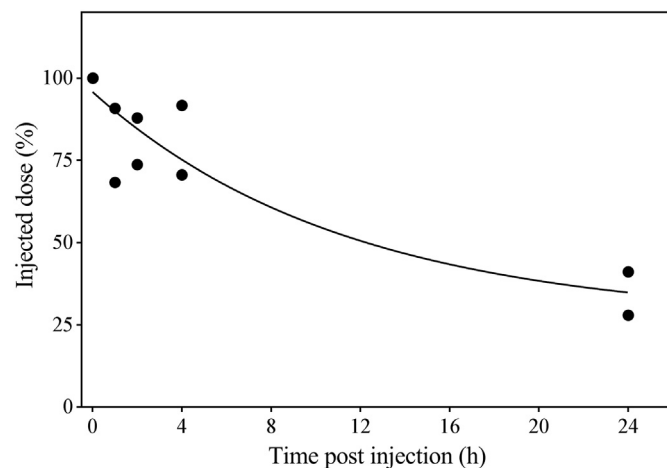
Fig. 3. Plasma levels of liposomes *in vivo*. Alexa750 labeled liposomes were injected intravenously. Blood was collected at 1 min (100% injection value $n = 4$), and 1 h, 2 h, 4 h and 24 h ($n = 2$) after i.v. injection. Plasma was separated from blood cells and fluorescence was measured by Odyssey fluorescence scanner.

liposomes, blood was collected to determine 100% injected dose (1 min time point). At 1, 2, 4 and 24 h post injection, percentage of the injected dose showed a gradual clearance in line with the long-circulating liposome design (Fig. 3).

$t_{1/2}$ of LCL-Alexa was estimated to be around 17 h in this mouse model. Fluorescence analysis was performed in whole organs and tumor bearing scaffolds after excision at 4 and 24 h post injection of LCL-Alexa. Fluorescence was detected in tumor scaffolds, which increased over time (Fig. 4A). Organs that are usually involved in liposomal clearance from the circulation such as liver, and spleen also showed high fluorescence (Fig. 4A). Surprisingly, a high fluorescence signal was observed in the kidneys and highly vascularized organs such as heart and lungs. Fig. 4B shows the results of quantitative fluorescence analysis in homogenized scaffolds and tissues by Odyssey fluorescence detector reflecting the whole tissue distribution pattern. Liposome accumulation in scaffolds and tissues was further analyzed in $5\,\mu$m cryosections using fluorescence microscopy (Fig. 4C), which corresponded to the fluorescence images from the same tissues using the Photon Imager and Odyssey fluorescence detector (Fig. 4A and B respectively). Most pronounced staining was found in the Kuppfer cells of the liver and the red pulp of the spleen.

Fig. 2. *In vitro* cytotoxicity of Free-DEX and LCL-DEX. MM.1S cells were incubated with a concentration range of Free-DEX ($n = 4$) and LCL-DEX ($n = 3$) for 48 h. Luminescence signals were determined 10 min after luciferin was added. Percentage viability was calculated using untreated cells as controls (100% viability). Data is expressed as mean $\pm$ SD.
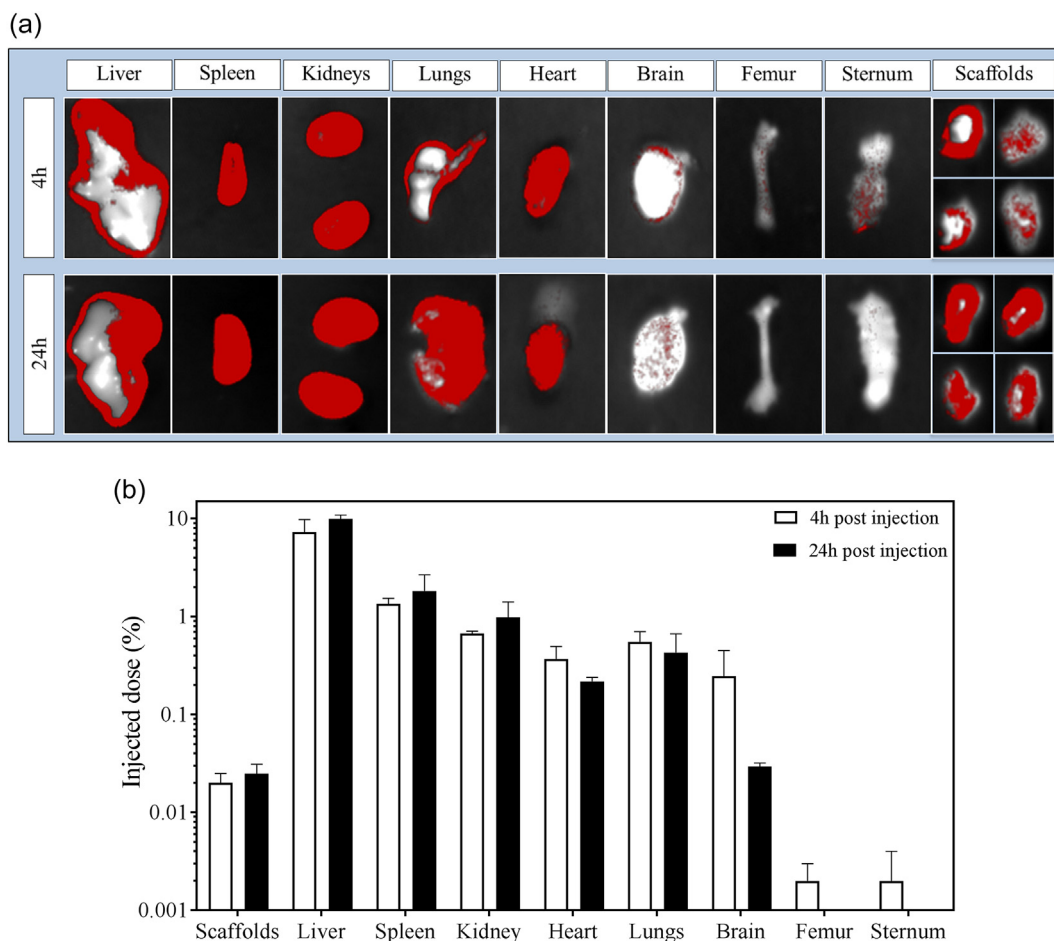
(a)

(b)

Fig. 4. *In vivo* localization of liposomes in tumor-bearing scaffolds and other tissues.

(A) Alexa750 labeled liposomes were injected intravenously (400 μg Alexa750/kg) at day 12 into mice bearing four MM.1S-inoculated scaffolds. Mice were sacrificed 4 h and 24 h after administration of liposomes, scaffolds and tissues were excised and imaged using Biospace Lab Photon Imager. Besides the above shown plasma residence, accumulation of liposomes could be detected in tumor bearing scaffolds and most organs. The non-fluorescent middle part of the liver is due to over-exposure of the signals and not due to absence of fluorescence. The threshold was set to a level to visualize the low fluorescence in tissues such as brain, femur, sternum, and scaffolds. (B) Accumulation of liposomes in scaffolds and other organs at 4 h and 24 h. Scaffolds and pieces of the frozen tissues were weighed and homogenized in RIPA buffer. Homogenates were vortexed and centrifuged. Fluorescence was detected in the supernatants by using Odyssey fluorescence scanner. Amount of Alexa750 fluorescence was determined by plotting fluorescence values in the calibration curve prepared by known concentrations of Alexa750 liposomes in the samples. Percentage of injected dose was estimated considering the plasma concentration at 1 min as 100%. (C) Alexa750 labeled liposomes were detected by fluorescence microscopy. Tissues collected and snap frozen 24 h after iv injection of Alexa750-labeled liposomes. All images taken at 60× magnification and processed using ImageJ. Blue (HOECHST 33342) = nuclei, green (Phalloidin-Alexa488) = Actin cytoskeleton, and red (Alexa750) = liposomes.

3.4. In vivo efficacy of LCL-DEX

Tumor scaffold bearing mice received five injections twice weekly with vehicle (PBS or PBS-liposomes), Free-DEX (1 and 4 mg/kg) and LCL-DEX (1 and 4 mg/kg). Tumor growth was monitored by BLI up to day 28 from start of the treatment. The PBS-control group was followed up to day 21 as some of the animals reached humane end point (i.e. cumulative tumor volume > 10% of body weight). Analysis of tumor cell growth by BLI indicates that LCL-DEX showed significant inhibition of tumor growth at 4 mg/kg compared to PBS control and PBS-liposome control groups, while free drug was ineffective at the same dose level (Fig. 5A). During the treatment period (up to day 14), a remarkable inhibition was seen in the LCL-DEX 4 mg/kg treated animals. The tumors started to grow after cessation of the treatment (Fig. 5B).

There was no significant tumor growth inhibition in either the 1 mg/kg Free-DEX or 1 mg/kg LCL-DEX groups, indicative of a steep dose response effect in case of LCL-DEX (Fig. 5B). The tumor doubling time calculated using the exponential growth equation was 4.8 days (95% CI = 4.4–5.5) for the PBS control group, 5.4 days (95% CI = 5.2–5.7) for PBS-liposomes treated group, 5.2 days (95%

CI = 4.7–6.0) for Free-DEX 1 mg/kg, 5.6 days (95% CI = 5.4–5.8) for LCL-DEX 1 mg/kg, 4.7 days (95% CI = 4.3–5.2) for Free-DEX 4 mg/kg, and 9.0 days (95% CI = 8.2–10.3) for LCL-DEX 4 mg/kg. Graphs of time vs BLI signals and time vs percentage tumor growth in individual animals (relative to day 0) are depicted in Supplemental Figs. 1 and 2 respectively. Approximately a maximum of 15% body weight reduction was observed in the LCL-DEX 4 mg/kg group. However, the body weight reduction was reversible after the treatment was stopped (Fig. 6).

4. Discussion

Complete recovery from multiple myeloma remains challenging as > 90% patients relapse or become refractory to treatment [37]. The reason for this lies at least partly in the absence of specificity of available drugs towards the target site, causing off-target adverse effects resulting in toxicities and dose-limited treatment regimens [14]. GCs are widely used in the clinic for the treatment of hematological malignancies including multiple myeloma. GCs have shown to exert anti-tumor activity by modulating the tumor microenvironment
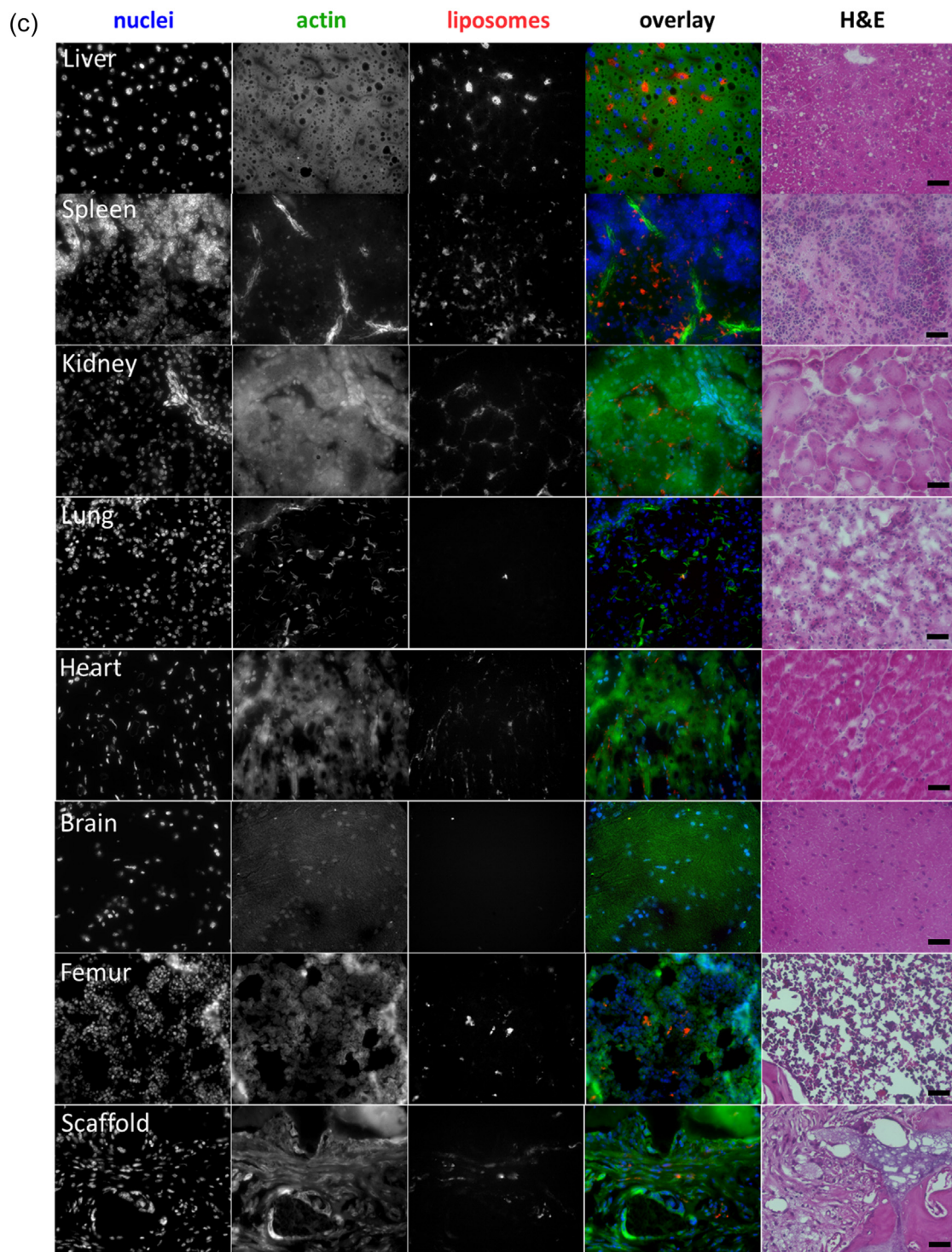
Fig. 4. (*continued*)

through anti-inflammatory effects and induction of myeloma cell apoptosis. *In vitro* efficacy of dexamethasone has been shown in myeloma cells by inducing transactivation of the glucocorticoid response element (GRE), and subsequently nuclear factor kappa B (NF-κB) transrepression, RAFTK phosphorylation and Bim induction [38]. Combination of GCs with other chemotherapeutics has been shown to lead to better clinical outcomes in inflammation-driven disorders and a variety of cancers including multiple myeloma [39]. Nanoformulations of GCs improve the therapeutic index by changing their pharmacokinetic, pharmacodynamic and toxicity profiles [29,40]. Liposomal drug

delivery has been validated to improve anti-inflammatory, as well as antitumor efficacy of glucocorticoids *in vivo* [41]. Liposomal GCs have been studied in various animal models of inflammation-driven diseases including rheumatoid arthritis [36,42–44], acute lung injury [45,46], asthma, encephalomyelitis, and uveitis [41,47] and cancer. Liposomal encapsulation substantially improved antitumor efficacy of GCs in animal models of colon carcinoma [6], melanoma [3,48,49], spontaneous breast carcinoma [2], prostate cancer [33,50], and sarcoma [51]. In hematological malignancies such as multiple myeloma, improved clinical outcomes with liposomal formulation of doxorubicin
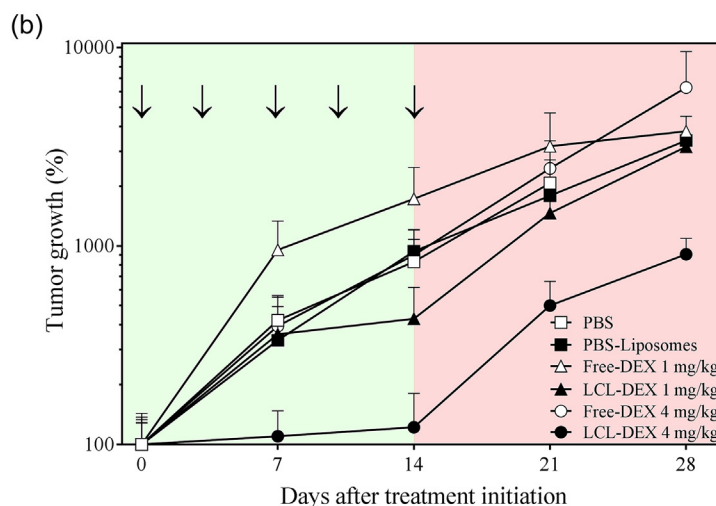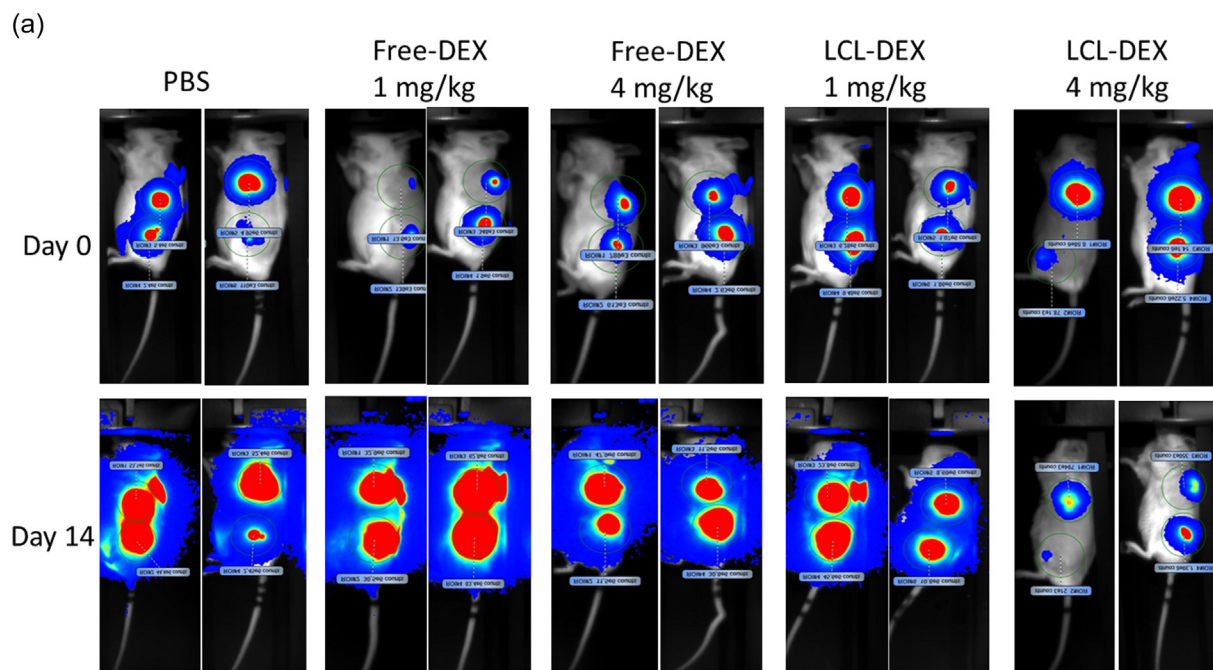
Fig. 5. *In vivo* efficacy of liposomal dexamethasone. Mice were inoculated with luciferase-marked MM.1S cells into the human bone containing scaffolds. Twelve days after tumor cells inoculation, animals were treated with PBS, PBS-liposomes, free dexamethasone (1 and 4 mg/kg) and liposomal dexamethasone (1 and 4 mg/kg). All treatments were given twice weekly via the tail vein, total of 5 injections. Bioluminescence imaging (BLI) was performed weekly. (A) BLI images of representative mice, before (Day 0; top panels) and 2 weeks after treatment initiation (Day 14; bottom panels). Circles indicate region of interest (ROI) for each individual scaffold. (B) BLI images were analyzed to obtain luminescence intensity as counts per min/square centimeters (cpm/cm^2). Percentage tumor growth was calculated relative to day 0. Statistical analysis was performed using nonlinear regression using exponential growth equation. The PBS group is excluded at the last time point (day 28) because humane end point was reached in some animals (tumor volume > 10% of body weight). Tumor growth rate was only reduced for the liposomal dexamethasone treatment regimen of 4 mg/kg compared to all other treatment groups. Arrows represent treatment days. Data is presented as mean ± SEM.

(Lipodox®/Doxil®/Caelyx®) combined with other drugs argue for developing liposomal formulations of other potent drug molecules such as GCs. Especially since GCs are already part of the majority of myeloma treatment protocols. Liposomal formulations of dexamethasone have so far not been evaluated (pre-)clinically. The difficulty to properly study the added value of nanomedicines in multiple myeloma pre-clinically lies partly in developing a predictive *in vivo* model of multiple myeloma that resembles the BM microenvironment and the involvement of the myeloma-stroma alliance. Both are key features in myeloma cell survival and disease progression [29,52,53]. Previously, we have described the development of an advanced human-mouse hybrid model of multiple myeloma. This model, containing a human BM-like microenvironment allowing for tumor-stroma interactions, has shown to

fatefully recapitulate MM and proven to be of translational value [30,54–56]. Because of this high translational value, we evaluated liposomal drug delivery for MM in this model. First, circulation and biodistribution of fluorescently labeled PEGylated liposomes (LCL-Alexa) was assessed. The half-life ($t_{1/2}$) resembled the profile of long circulating PEG-liposomes (approximately 17 h in this model). Interestingly, these values are higher than in immunocompetent mouse strains tested earlier [6]. In previous studies, we have reported that approximately 60% and 15% of the injected dose of ^{111}In-labeled liposomes was present at 6 h and 24 h post injection in C57BL/6 and BALB/c mice, respectively. The higher plasma concentration of liposomes in immunocompromised $RAG2^{-/-}\gamma c^{-/-}$ mice used in the present study is likely due to the lack of most of the immune system in this
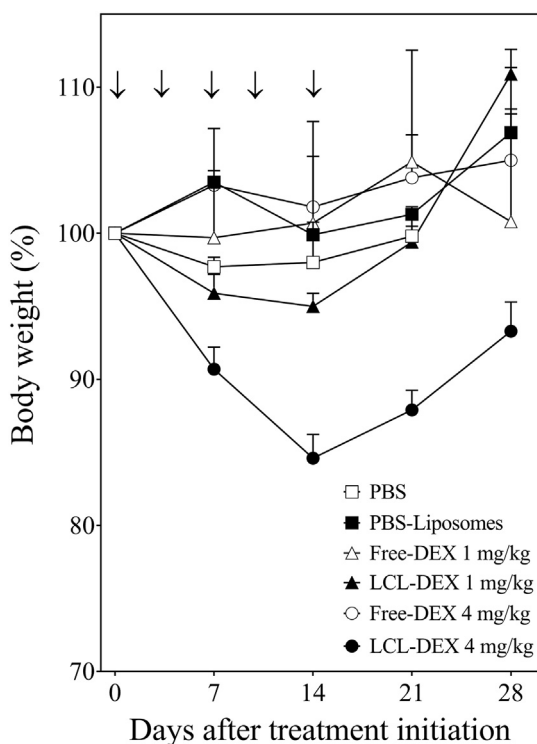
Fig. 6. Body weight measurements. As an estimate of overall well-being, changes in body weight of animals in all experimental groups was monitored. Liposomal dexamethasone at 4 mg/kg was the only group showing a reduction in body weight of DEX-treated animals. However, the body weight reduction was reversible after the treatment was stopped. Arrows represent treatment days. Data is presented as mean ± SD.

strain since RAG2$^{-/-}$γc$^{-/-}$ mice lack T cells, B cells and NK cells but do have tissue macrophages [57]. We have previously evaluated the liposomal formulation of dexamethasone for *in vitro* and *in vivo* release kinetics [58,59]. *In vitro*, the formulation was found to be stable, releasing merely 5% the encapsulated drug over a period of 2 weeks at 37 °C [58]. *In vivo*, plasma concentrations of liposomal-encapsulated and non-encapsulated glucocorticoids were determined in rats. Liposomal formulations of dexamethasone, prednisolone, and budesonide showed similar plasma levels of encapsulated drug. The free drug concentration in plasma, however, was higher in case of dexamethasone formulation [59]. Fluorescence imaging of tumor scaffolds showed liposome accumulation, which is likely a result of the EPR effect. Importantly, fluorescence intensity in the scaffolds was slightly higher at 24 h when compared to 4 h post injection, implying that liposomal accumulation is increasing in time. It is important to mention here that the biodistribution experiment was performed on day 12 after myeloma cells inoculation, which is still a very early time point in the tumor development. As expected, high liposome accumulation was observed in macrophage-rich organs liver, spleen and lungs. Surprisingly, there was also accumulation seen in the kidneys and heart in this model. A plausible explanation of higher kidney accumulation could be renal inflammation. Renal inflammation is one of the pathophysiologic events in multiple myeloma due to local accumulation of antibody light chains [60,61]. The increased fluorescence signal in highly vascularized tissues such as heart and lungs is likely due to contamination of blood as in the fluorescence microscopy images of tissue sections, the signals were not evident. Accumulation in the brain and femur was negligible as was expected for tissues with an intact endothelial barrier. In the 4 h tissue homogenates analyzed by Odyssey fluorescence scanner (Fig. 4B), the brain tissue shows somewhat higher fluorescence signal, which is not depicted in the images of whole organs (Fig. 4A). This could be due to substantial variation between the two animals at this

time point, hence the large standard error. Supplemental Fig. 3 shows whole organ fluorescence images of individual mice. *In vitro*, Free-DEX and LCL-DEX showed a concentration dependent anti-myeloma effect up to 2 μM for the MM1.S cell line. The higher IC$_{50}$ values for LCL-DEX can be explained by the fact that liposomes may have to be taken up by the cells and dexamethasone has to be released in order to exert its effect to the cells.

The *in vivo* anti-myeloma efficacy of LCL-DEX was evaluated in the humanized mouse model inoculated with MM1.S cells, and was compared with Free-DEX at equivalent doses (i.e. 1 and 4 mg/kg). Bioluminescence imaging was performed to monitor and quantify tumor growth, and showed a strong growth inhibition in LCL-DEX treated animals at a dose of 4 mg/kg (vs. the other treatment groups). Strikingly, no tumor growth inhibition was observed in Free-DEX treated animals at the same dose level. Importantly, dexamethasone in the free from is reported to have antitumor efficacy at a dose regimen 1 mg/kg [62,63]. However, it is important to note that a different doing frequency was used in these studies (five times weekly, compared to two times weekly in our study). Moreover, the above mentioned studies were performed in subcutaneous xenograft models. The interaction of the myeloma cells with the bone microenvironment may have impact on the efficacy of the drug, leading to resistance. This might be a plausible explanation why 4 mg/kg of free dexamethasone was ineffective in our model. Finally, the overall systemic toxicity related to the treatment was evaluated by monitoring body weights of the animals. LCL-DEX given at the highest dose level of 4 mg/kg showed up to ~15% loss in body weight during the course of treatment. However, this loss in body weight was reversible after the treatment was finished. Earlier studies have been shown similar effects on body weight upon LCL-DEX treatment. Repeated administration of free or liposomal dexamethasone in rats resulted in significant body weight reduction [33]. However, this decrease in body weight could be related to known effects of exogenous corticosteroid exposure and no unexpected adverse effects were observed that could be attributable to administering dexamethasone in the liposomal rather than in free form. The somewhat higher body weight reduction with LCL-DEX treatment in the present study may related to the longer circulation time of the liposomes, and thus dexamethasone in this mouse model, resulting in higher exposure to the macrophage-rich organs.

To our knowledge, this is the first time that the *in vivo* efficacy of liposomal dexamethasone is evaluated as a monotherapy in multiple myeloma using a clinically predictive mouse model. The results indicate that liposomal encapsulation can improve the therapeutic index of dexamethasone by improving pharmacokinetic and pharmacodynamic properties. By using liposomal formulations, it is likely that a lower dose of dexamethasone could be used in currently available combination regimens in clinical settings, which could improve therapeutic outcomes and reduce dose-related side effects. Further research is warranted to evaluate liposome-encapsulated dexamethasone as a part of the existing treatment regimens or as a monotherapy for multiple myeloma.

Supplementary data to this article can be found online at https:// doi.org/10.1016/j.jconrel.2019.01.028.

Conflict of interest

References

[1] G.R. Mehta, et al., Multiple myeloma, Dis. Mon. 60 (10) (2014) 483–488.

[2] A.K. Deshantri, et al., Liposomal prednisolone inhibits tumor growth in a spontaneous mouse mammary carcinoma model, J. Control. Release 243 (2016) 243–249.

[3] M. Banciu, et al., Antitumor activity of liposomal prednisolone phosphate depends on the presence of functional tumor-associated macrophages in tumor tissue, Neoplasia 10 (2) (2008) 108–117.

[4] M. Banciu, et al., Utility of targeted glucocorticoids in cancer therapy, J. Liposome Res. 18 (1) (2008) 47–57.

[5] M. Ciampricotti, et al., Chemotherapy response of spontaneous mammary tumors is independent of the adaptive immune system, Nat. Med. 18 (3) (2012) 344–346 (author reply 346).

[6] R.M. Schiffelers, et al., Liposome-encapsulated prednisolone phosphate inhibits growth of established tumors in mice, Neoplasia 7 (2) (2005) 118–127.

[7] C. Stahn, F. Buttgereit, Genomic and nongenomic effects of glucocorticoids, Nat. Clin. Pract. Rheumatol. 4 (10) (2008) 525–533.

[8] J.M. Metselaar, G. Storm, Liposomes in the treatment of inflammatory disorders, Expert Opin. Drug Deliv. 2 (3) (2005) 465–476.

[9] S.J. Grethlein, Multiple Myeloma Treatment Protocols, Medscape, 2016.

[10] D.S. Siegel, et al., Improvement in overall survival with carfilzomib, lenalidomide, and dexamethasone in patients with relapsed or refractory multiple myeloma, J. Clin. Oncol. 36 (8) (2018) 728–734.

[11] T. Facon, et al., Final analysis of survival outcomes in the phase 3 FIRST trial of upfront treatment for multiple myeloma, Blood 131 (3) (2018) 301–310.

[12] D.M. Weber, et al., Lenalidomide plus dexamethasone for relapsed multiple myeloma in North America, N. Engl. J. Med. 357 (21) (2007) 2133–2142.

[13] M. Das, Lenalidomide plus dexamethasone in multiple myeloma, Lancet Oncol. 19 (1) (2018) e12.

[14] B. Ozbakir, et al., Liposomal corticosteroids for the treatment of inflammatory disorders and cancer, J. Control. Release 190 (2014) 624–636.

[15] R.M. Schiffelers, et al., Therapeutic application of long-circulating liposomal glucocorticoids in auto-immune diseases and cancer, J. Liposome Res. 16 (3) (2006) 185–194.

[16] R.F. Laan, T.L. Jansen, P.L. van Riel, Glucocorticosteroids in the management of rheumatoid arthritis, Rheumatology (Oxford) 38 (1) (1999) 6–12.

[17] M.D. Howard, et al., Nanocarriers for vascular delivery of anti-inflammatory agents, Annu. Rev. Pharmacol. Toxicol. 54 (2014) 205–226.

[18] U. Bulbake, et al., Liposomal formulations in clinical use: an updated review, Pharmaceutics 9 (2) (2017).

[19] J.E. Lancet, et al., Final results of a phase III randomized trial of CPX-351 versus 7 + 3 in older patients with newly diagnosed high risk (secondary) AML, J. Clin. Oncol. 34 (15_suppl) (2016) 7000.

[20] H. Maeda, H. Nakamura, J. Fang, The EPR effect for macromolecular drug delivery to solid tumors: Improvement of tumor uptake, lowering of systemic toxicity, and distinct tumor imaging *in vivo*, Adv. Drug Deliv. Rev. 65 (1) (2013) 71–79.

[21] M.T. Cibeira, et al., Bone marrow angiogenesis and angiogenic factors in multiple myeloma treated with novel agents, Cytokine 41 (3) (2008) 244–253.

[22] S. Kumar, et al., Effect of thalidomide therapy on bone marrow angiogenesis in multiple myeloma, Leukemia 18 (3) (2004) 624–627.

[23] A. Dmoszynska, et al., The influence of thalidomide therapy on cytokine secretion, immunophenotype, BCL-2 expression and microvessel density in patients with resistant or relapsed multiple myeloma, Neoplasma 52 (2) (2005) 175–181.

[24] C.S. Mitsiades, et al., The role of the bone microenvironment in the pathophysiology and therapeutic management of multiple myeloma: interplay of growth factors, their receptors and stromal interactions, Eur. J. Cancer 42 (11) (2006) 1564–1573.

[25] C.S. Mitsiades, et al., Focus on multiple myeloma, Cancer Cell 6 (5) (2004) 439–444.

[26] D.S. Krause, D.T. Scadden, A hostel for the hostile: the bone marrow niche in hematologic neoplasms, Haematologica 100 (11) (2015) 1376–1387.

[27] S. Manier, et al., Bone marrow microenvironment in multiple myeloma progression, J. Biomed. Biotechnol. 2012 (2012) 157496.

[28] C. Tripodo, et al., The bone marrow stroma in hematological neoplasms–a guilty bystander, Nat. Rev. Clin. Oncol. 8 (8) (2011) 456–466.

[29] A.K. Deshantri, et al., Nanomedicines for the treatment of hematological malignancies, J. Control. Release 287 (2018) 194–215.

[30] R.W. Groen, et al., Reconstructing the human hematopoietic niche in immunodeficient mice: opportunities for studying primary multiple myeloma, Blood 120 (3) (2012) e9–e16.

[31] H.J. Prins, et al., Bone-forming capacity of mesenchymal stromal cells when cultured in the presence of human platelet lysate as substitute for fetal bovine serum, Tissue Eng. Part A 15 (12) (2009) 3741–3751.

[32] B. Theek, et al., Sonoporation enhances liposome accumulation and penetration in tumors with low EPR, J. Control. Release 231 (2016) 77–85.

[33] J. Kroon, et al., Liposomal delivery of dexamethasone attenuates prostate cancer bone metastatic tumor growth *in vivo*, Prostate 75 (8) (2015) 815–824.

[34] C. Jaafar-Maalej, et al., Ethanol injection method for hydrophilic and lipophilic drug-loaded liposome preparation, J. Liposome Res. 20 (3) (2010) 228–243.

[35] V. Joguparthi, T.X. Xiang, B.D. Anderson, Liposome transport of hydrophobic drugs: gel phase lipid bilayer permeability and partitioning of the lactone form of a hydrophobic camptothecin, DB-67, J. Pharm. Sci. 97 (1) (2008) 400–420.

[36] J.M. Metselaar, et al., Complete remission of experimental arthritis by joint targeting of glucocorticoids with long-circulating liposomes, Arthritis Rheum. 48 (7) (2003) 2059–2066.

[37] P. de la Puente, A.K. Azab, Nanoparticle delivery systems, general approaches, and their implementation in multiple myeloma, Eur. J. Haematol. 98 (6) (2017) 529–541.

[38] S. Sharma, A. Lichtenstein, Dexamethasone-induced apoptotic mechanisms in myeloma cells investigated by analysis of mutant glucocorticoid receptors, Blood 112 (4) (2008) 1338–1345.

[39] A.K. Nooka, S. Lonial, Novel Combination Treatments in Multiple Myeloma, Oncology (Williston Park) 30 (5) (2016) 451–465.

[40] F. Buttgereit, J.W.J. Bijlsma, C. Strehl, Will we ever have better glucocorticoids? Clin. Immunol. 186 (2018) 64–66.

[41] F. Luhder, H.M. Reichardt, Novel drug delivery systems tailored for improved administration of glucocorticoids, Int. J. Mol. Sci. 18 (9) (2017).

[42] G.A. Koning, et al., Targeting of angiogenic endothelial cells at sites of inflammation by dexamethasone phosphate-containing RGD peptide liposomes inhibits experimental arthritis, Arthritis Rheum. 54 (4) (2006) 1198–1208.

[43] M. Jia, et al., A novel dexamethasone-loaded liposome alleviates rheumatoid arthritis in rats, Int. J. Pharm. 540 (1–2) (2018) 57–64.

[44] W. Hofkens, et al., Liposomal targeting of glucocorticoids to the inflamed synovium inhibits cartilage matrix destruction during murine antigen-induced arthritis, Int. J. Pharm. 416 (2) (2011) 486–492.

[45] M.A. Hegeman, et al., Liposome-encapsulated dexamethasone attenuates ventilator-induced lung inflammation, Br. J. Pharmacol. 163 (5) (2011) 1048–1058.

[46] Z.E. Suntres, P.N. Shek, Prophylaxis against lipopolysaccharide-induced lung injuries by liposome-entrapped dexamethasone in rats, Biochem. Pharmacol. 59 (9) (2000) 1155–1161.

[47] C.W. Wong, et al., Evaluation of subconjunctival liposomal steroids for the treatment of experimental uveitis, Sci. Rep. 8 (1) (2018) 6604.

[48] M. Banciu, et al., Anti-angiogenic effects of liposomal prednisolone phosphate on B16 melanoma in mice, J. Control. Release 113 (1) (2006) 1–8.

[49] M. Banciu, et al., Liposomal glucocorticoids as tumor-targeted anti-angiogenic nanomedicine in B16 melanoma-bearing mice, J. Steroid Biochem. Mol. Biol. 111 (1–2) (2008) 101–110.

[50] J. Kroon, et al., Liposomal nanomedicines in the treatment of prostate cancer, Cancer Treat. Rev. 40 (4) (2014) 578–584.

[51] J. Sun, et al., Evaluation of the antitumor effect of dexamethasone palmitate and doxorubicin co-loaded liposomes modified with a sialic acid-octadecylamine conjugate, Eur. J. Pharm. Sci. 93 (2016) 177–183.

[52] T. Hideshima, et al., Understanding multiple myeloma pathogenesis in the bone marrow to identify new therapeutic targets, Nat. Rev. Cancer 7 (8) (2007) 585–598.

[53] S.K. Kumar, et al., Multiple myeloma, Nat. Rev. Dis. Primers 3 (2017) 17046.

[54] E. Drent, et al., Pre-clinical evaluation of CD38 chimeric antigen receptor engineered T cells for the treatment of multiple myeloma, Haematologica 101 (5) (2016) 616–625.

[55] I.S. Nijhof, et al., Upregulation of CD38 expression on multiple myeloma cells by all-trans retinoic acid improves the efficacy of daratumumab, Leukemia 29 (10) (2015) 2039–2049.

[56] I.S. Nijhof, et al., Preclinical evidence for the therapeutic potential of CD38-targeted immuno-chemotherapy in multiple myeloma patients refractory to lenalidomide and bortezomib, Clin. Cancer Res. 21 (12) (2015) 2802–2810.

[57] F. Mazurier, et al., A novel immunodeficient mouse model—RAG2 x common cytokine receptor gamma chain double mutants—requiring exogenous cytokine administration for human hematopoietic stem cell engraftment, J. Interf. Cytokine Res. 19 (5) (1999) 533–541.

[58] L. Quan, et al., Nanomedicines for inflammatory arthritis: head-to-head comparison of glucocorticoid-containing polymers, micelles, and liposomes, ACS Nano 8 (1) (2014) 458–466.

[59] J.M. van den Hoven, et al., Optimizing the therapeutic index of liposomal glucocorticoids in experimental arthritis, Int. J. Pharm. 416 (2) (2011) 471–477.

[60] S.T. Lwin, C.M. Edwards, R. Silbermann, Preclinical animal models of multiple myeloma, Bonekey Rep. 5 (2016) 772.

[61] A. Davenport, G. Merlini, Myeloma kidney: advances in molecular mechanisms of acute kidney injury open novel therapeutic opportunities, Nephrol. Dial. Transplant. 27 (10) (2012) 3713–3718.

[62] G. Rozic, et al., STK405759 as a combination therapy with bortezomib or dexamethasone, in *in vitro* and *in vivo* multiple myeloma models, Oncotarget 9 (59) (2018) 31367–31379.

[63] E.M. Ocio, et al., *In vitro* and *in vivo* rationale for the triple combination of panobinostat (LBH589) and dexamethasone with either bortezomib or lenalidomide in multiple myeloma, Haematologica 95 (5) (2010) 794–803.